Progress In Electromagnetics Research C, Vol. 20, 67–81, 2011

DESIGN AND ANALYSIS OF DUAL-FREQUENCY MODIFIED 3-WAY BAGLEY POWER DIVIDERS

A. Qaroot, K. Shamaileh, and N. Dib

Electrical Engineering Department
Jordan University of Science and Technology
P. O. Box 3030, Irbid 22110, Jordan

Abstract—In this paper, different topologies of dual-frequency modified 3-way Bagley polygon power dividers are designed and analyzed. Equal split power division is achieved at arbitrary design frequencies. In the first structure, two-section transmission line transformer is used to realize the dual-frequency operation. In the second and third structures, dual-frequency T-shaped and π-shaped matching networks are used. For the sake of simplicity, closed form design equations are presented for each matching network. To validate the design procedure, three examples are designed, simulated, and fabricated. The three matching networks are explored through these three examples. The design frequencies are chosen to be 0.5 GHz and 1 GHz.

1. INTRODUCTION

With the advent of new wireless communication technologies, multi-frequency microwave components are widely needed. In this regard, multi-frequency transmission line transformers (TLTs) have been reported in literature [1–4]. In [1], closed form design equations for the dual-frequency TLT were presented. Tri-frequency and quad-frequency TLTs were reported in [2, 3], respectively. Furthermore, the general design of multi-frequency TLTs for arbitrary number of operating frequencies was presented in [4]. On the other hand, other dual-frequency matching networks, namely T-shaped and π-shaped matching networks were presented in [5, 6].

The Wilkinson power divider (WPD) is one of the devices that have taken advantage from the multi-frequency TLTs in microwave

Received 8 January 2011, Accepted 28 February 2011, Scheduled 2 March 2011
Corresponding author: Abdullah Mazen Qaroot (abd_mazen@hotmail.com).

components design. In [7], the design of dual-frequency unequal split WPD using Monzon's equations [1] was presented. In [8, 9], triple and quad-frequency equal split WPDs were designed and investigated. The general design of multi-frequency equal split WPD was presented in [10]. In [11], the multi-frequency operation was extended to the unequal split WPD. Moreover, many papers addressed the design of dual-frequency WPDs and branch line couplers [12–20].

The Bagley polygon power divider is another planar microwave divider that has lately attracted some attention [21–25]. Compared to the WPD, the Bagley power divider (BPD) does not require any lumped elements, and can be easily extended to any number of output ports. On the other hand, the isolation performance between output ports is not as good as that of the WPDs [21–25]. In [21], reduced size multi-way Bagley power divider (BPD), using open stubs was presented. In [22], an optimum design of a modified 3-way Bagley rectangular power divider was presented. In [23], a general design of compact multi-way dividers based on BPDs was introduced. In [24], a compact dual-frequency 3-way BPD using composite right/left handed (CRLH) transmission lines was implemented. However, parallel combinations of lumped elements (capacitors and inductors) were considered. Very recently, dual-passband filter section based on the generalized Bagley polygon four-port power divider was presented in [25].

In this paper, based on the modified BPD proposed in [23], dual-frequency 3-way BPDs will be investigated. The dual-frequency operation is achieved using three different techniques; namely dual-frequency TLT [1], T-shaped dual-frequency matching network [5], and π-shaped dual-frequency transformer [6]. The design procedure is simple and straightforward. After reducing the 3-way BPD to its equivalent circuit model, one of the dual-frequency matching networks can be used instead of the quarter-wave section to generate the dual-frequency operation of the BPD. Following the same procedure, triple and quad frequency operation can be achieved by utilizing the triple and quad TLTs [2, 3]. The designed dual-frequency dividers are simulated using two different full-wave simulators (HFSS [26] and IE3D [27]). Moreover, fabrication and measurement are performed. The results of the simulations and the measurements are in good agreement.

The paper is divided as follows: Section 2 presents the 3-way BPD and its equivalent circuit model; Section 3 presents the three matching networks and summarizes the equations used to design the three different dual-frequency transformers; Section 4 presents three examples along with the simulation results; Section 5 details the

fabricated circuits and shows the experimental results; and Section 6 concludes the paper.

2. 3-WAY BAGLEY POWER DIVIDER

As mentioned above, based on the conventional Bagley polygon power divider, compact modified Bagley dividers were proposed in [23]. Figure 1(a) shows the schematic diagram of the 3-way modified BPD [23]. Noting that this divider is symmetric around its center line, an equivalent circuit (looking from Port 1 to the right or left side) can be drawn as shown in Figure 1(b).

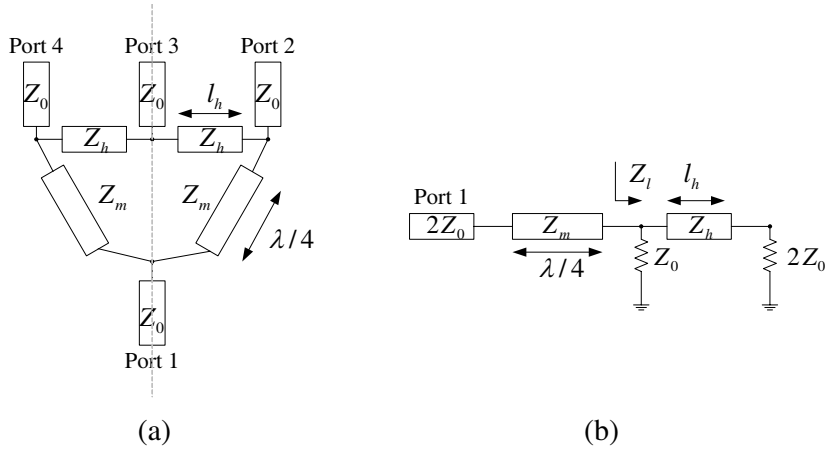

Figure 1. Schematic diagram of the 3-way modified BPD, and its equivalent circuit.

Referring to the equivalent circuit it can be easily realized that choosing $Z_h = 2Z_0$ makes the design of this BPD independent of the length l_h. In this case, the characteristic impedance (Z_m) of the quarter wave section is $Z_m = \sqrt{(2Z_0)\, Z_l}$, where $Z_l = \frac{2Z_0}{3}$. This gives:

$$Z_m = \frac{2Z_0}{\sqrt{3}} \tag{1}$$

Thus, each quarter-wave section matches an impedance of $\frac{2Z_0}{3}$ to $2Z_0$, resulting in a perfect match at port 1 (the input port) and equal split power division to the three output ports. As noted in the Introduction, the BPD does not contain any lumped elements, and it can be easily extended to any (odd) number of output ports. Besides the modified 3-way BPD, a 5-way modified BPD was presented in [23]. Here, we

concentrate on the design of dual-frequency 3-way modified BPDs, while the same techniques can be applied on the 5-way BPD.

3. DUAL-FREQUENCY MATCHING NETWORKS

3.1. Two-Section Transmission Line Transformer [1]

Figure 2 shows a schematic diagram for the dual-frequency two-section transmission line transformer (TLT) [1]. To achieve a dual-frequency operation, the conventional quarter-wave section is replaced by two transmission line sections, as shown in Figure 2.

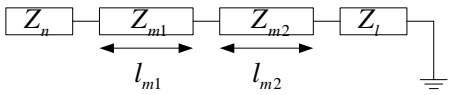

Figure 2. Dual-frequency two-section TLT.

The characteristic impedances (Z_{m1}, Z_{m2}) and the line lengths (l_{m1}, l_{m2}) for the two sections can be evaluated using the following equations [1]:

$$l_{m1} = l_{m2} \tag{2}$$

$$l_{m2} = \frac{\pi}{\beta_1 + \beta_2} \tag{3}$$

$$\alpha = (\tan(\beta_1 l_{m1}))^2 \tag{4}$$

$$Z_{m1} = \sqrt{\frac{Z_n}{2\alpha}(Z_l - Z_n) + \sqrt{\left[\frac{Z_n}{2\alpha}(Z_l - Z_n)\right]^2 + Z_n^3 Z_l}} \tag{5}$$

$$Z_{m2} = \frac{Z_n Z_l}{Z_{m1}} \tag{6}$$

where β_1 and β_2 are the phase constants at the design frequencies f_1 and f_2, respectively. In the case of the 3-way BPD, Z_n corresponds to $2Z_0$, while $Z_l = \frac{2Z_0}{3}$, where Z_0 is the ports' impedance (usually 50 Ω).

3.2. T-Shaped Matching Network [5]

In this topology, the quarter wavelength section shown in Figure 3(a) is replaced by a dual-frequency T-shaped transmission lines network (with an open stub). The equivalency between the transmission line section shown in Figure 3(a) and the T-shaped network in Figure 3(b) is investigated depending on the *ABCD* matrices of both networks [5].

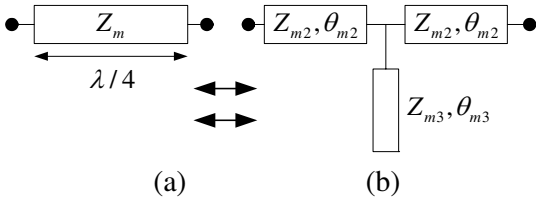

Figure 3. (a) Quarter-wave transmission line. (b) Equivalent T-shaped transmission line.

Equating the elements of both $ABCD$ matrices and using simple trigonometric identities lead to the following design equations [5]:

$$\theta_{m2(f_1)} = \frac{\pi}{p+1} \tag{7}$$

$$\theta_{m2(f_2)} = p\theta_{m2(f_1)} \tag{8}$$

$$\theta_{m3(f_1)} = \frac{2\pi}{p+1} \tag{9}$$

where $\theta_{m2(f_1)}$ and $\theta_{m2(f_2)}$ are the electrical lengths at f_1 and f_2, respectively, $\theta_{m3(f_1)}$ is the electrical length of the open stub at f_1 and p is the frequency ratio (f_2/f_1). It should be mentioned here that Equations (7) and (9) are given for compact size transmission lines. Moreover, the values of the characteristic impedances Z_{m2} and Z_{m3} can be calculated using the following equations [5]:

$$Z_{m2} = \frac{Z_m}{\tan\theta_{m2(f_1)}} \tag{10}$$

$$Z_{m3} = 0.5Z_{m2}\tan^2\theta_{m3(f_1)} \tag{11}$$

3.3. π-Shaped Matching Network [6]

The π-shaped dual-frequency transformer is shown in Figure 4. Two open stubs with characteristic impedances Z_{m2} and Z_{m3}, and electrical lengths θ_{m2} and θ_{m3}, respectively, are used besides the section with characteristic impedance of Z_{m1} and electrical length θ_{m1}. The closed

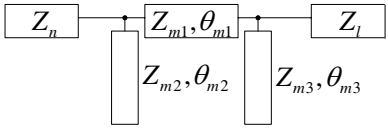

Figure 4. π-shaped dual-frequency transformer.

form design equations were derived in [6] by solving the matching equations. It should be pointed out that the dual-frequency π-shaped transformer has infinite number of solutions.

One of the solutions of interest is in which compact lengths and high aspect ratio (W/h) are achieved (where W is the microstrip line width and h is the substrate thickness). High aspect ratio means that the characteristic impedances of the three sections (Z_{m1}, Z_{m2}, and Z_{m3}) are not too high. Based on the preceding idea, the closed form design equations are chosen to be [6]:

$$l_{m3} = l_{m1} = l_{m2} \tag{12}$$

$$Z_{m1} = Z_n\sqrt{k} \tag{13}$$

$$Z_{m2} = Z_n\frac{\alpha\sqrt{k}}{1+\sqrt{k}} \tag{14}$$

$$Z_{m3} = Z_n\frac{\alpha\cdot k}{1+\sqrt{k}} \tag{15}$$

where l_{m2} and α are given by Equations (3) and (4) respectively, and k is the normalized load impedance ($k = Z_l/Z_n$).

4. EXAMPLES AND SIMULATION RESULTS

Based on the dual-frequency matching networks presented in the previous section, three dual-frequency BPDs operating at 0.5 GHz and 1 GHz are designed, simulated, and fabricated. First, circuit models of the designed dual-frequency 3-way BPDs are analyzed using Ansoft Designer [26], and then, the proposed dividers are simulated using the full-wave simulators HFSS [26] and IE3D [27]. An FR-4 substrate, with a relative permittivity of $\varepsilon_r = 4.6$ and a substrate height of $h = 1.6$ mm is used. In the three examples presented below, the terminating impedance Z_0 is chosen to be $50\,\Omega$ which gives $Z_h = 100\,\Omega$ and $W_h = 0.64$ mm; while, l_h is chosen arbitrarily.

4.1. Example 1: Dual-Frequency BPD Using Two-Section TLT

Using the design Equations (5) and (6), the dual-frequency two-section TLT impedances are found to be: $Z_{m1} = 69.05\,\Omega$ and $Z_{m2} = 48.27\,\Omega$. The corresponding microstrip line widths considering the substrate mentioned above are $W_{m1} = 1.6$ mm and $W_{m2} = 3.11$ mm. From Equations (2) and (3), the electrical lengths are $l_{m1} = l_{m2} = 60^\circ$, where f_1 is the reference frequency. The corresponding physical lengths are

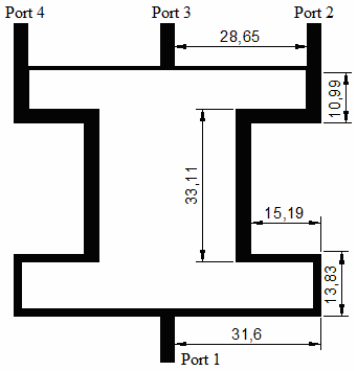

Figure 5. The layout of the designed dual-frequency BPD using TLT sections (All dimensions are in mm).

$l_{m1} = 55.19\,\text{mm}$ and $l_{m2} = 53.69\,\text{mm}$. Figure 5 represents the layout of the designed dual-frequency BPD using TLT sections.

Figure 6 presents the simulation results of this dual-frequency 3-way BPD. Dual-frequency operation with center frequencies around 0.5 GHz and 1 GHz is clearly seen. As shown in Figure 6(a), good input port matching is achieved with S_{11} below $-20\,\text{dB}$ at the design frequencies. Figures 6(b) and 6(c) show the transmission parameters (S_{12} and S_{13}). Since the BPD is an equal split power divider, the simulated values are close to the theoretical value of $-4.77\,\text{dB}$ at the design frequencies. The small differences are due to losses and discontinuities shown in Figure 5. It is worth mentioning here that because of the symmetry of the structure, S_{14} is the same as S_{12}.

4.2. Example 2: Dual-Frequency BPD Using T-Shaped Matching Network

Incorporating the dual frequency T-shaped matching network into the modified 3-way BPD and making use of Equations (7)–(11), the following design parameters are obtained: $Z_{m2} = 33.33\,\Omega$ and $Z_{m3} = 50\,\Omega$. Their corresponding microstrip line widths are $W_{m2} = 5.45\,\text{mm}$ and $W_{m3} = 2.94\,\text{mm}$, respectively. The electrical lengths of the designed sections are found to be $\theta_{m2(f_1)} = 60°$ and $\theta_{m3(f_1)} = 120°$, with physical lengths of $l_{m2} = 52.26\,\text{mm}$ and $l_{m3} = 107.66\,\text{mm}$, respectively. Figure 7 shows the layout of the designed dual-frequency 3-way BPD using the T-shaped matching network.

Figure 8 presents the simulation results of this dual-frequency 3-way BPD. Figure 8(a) shows that very good input port matching is

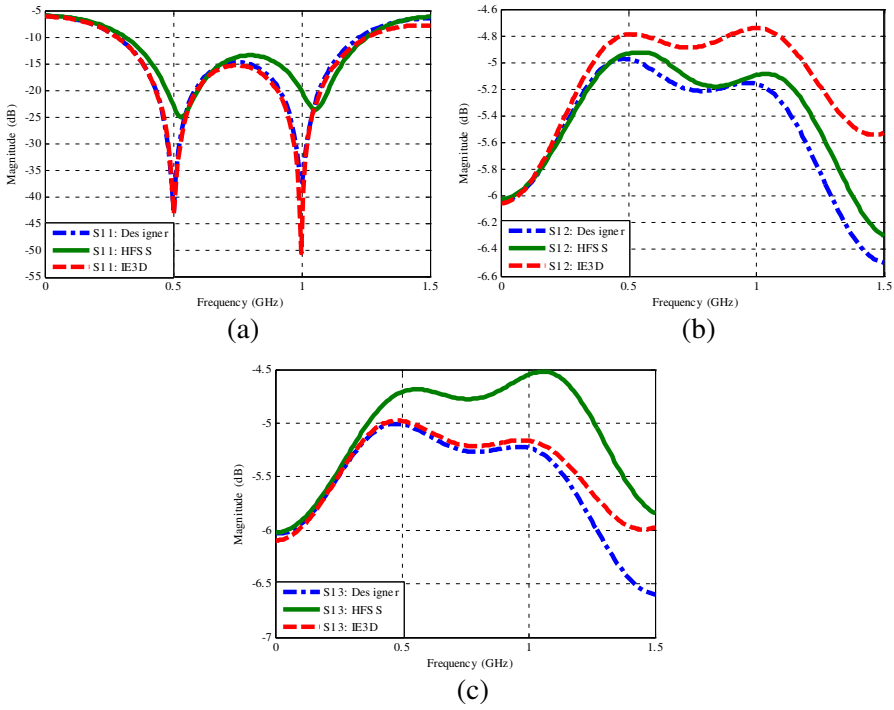

Figure 6. The simulation results for the dual-frequency 3-way BPD shown in Figure 5.

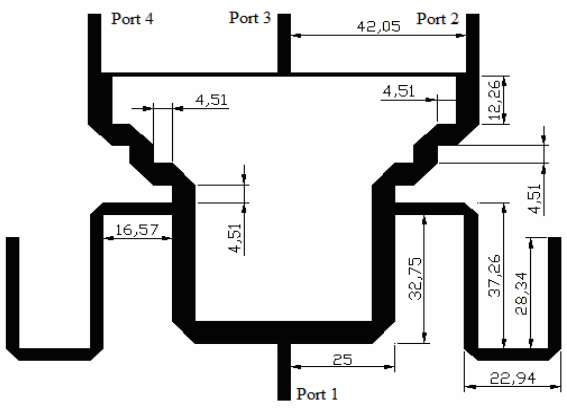

Figure 7. The layout of the designed dual-frequency BPD using T-shaped matching network (All dimensions are in mm).

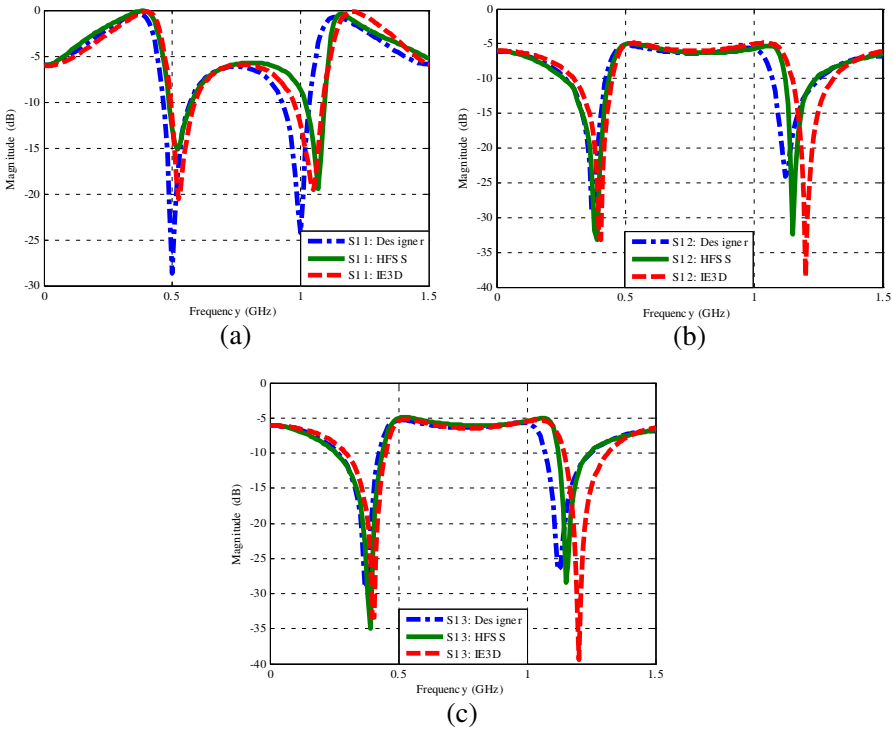

Figure 8. The simulation results for the dual-frequency BPD using T-shaped matching network.

obtained around the design frequencies, while Figures 8(b) and 8(c) show that the values of the transmission scattering parameters at the design frequencies are close to their theoretical value of $-4.77\,\text{dB}$.

4.3. Example 3: Dual-Frequency BPD Using π-Shaped Matching Network

In this example, the quarter-wave sections in the BPD are replaced by the π-shaped dual-frequency transformers. Using Equations (3), (4) and (12)–(15), the design parameters are found to be: $Z_{m1} = 57.73\,\Omega$, $Z_{m2} = 109.8\,\Omega$, and $Z_{m3} = 63.4\,\Omega$. The corresponding microstrip line widths are: $W_{m1} = 2.28\,\text{mm}$, $W_{m2} = 0.48\,\text{mm}$, and $W_{m3} = 1.9\,\text{mm}$, respectively. The electrical lengths are $l_{m1} = l_{m2} = l_{m3} = 60^\circ$ where f_1 is the reference frequency, and the corresponding physical lengths are $l_{m1} = 54.43\,\text{mm}$, $l_{m2} = 57.05\,\text{mm}$, and $l_{m3} = 54.83\,\text{mm}$, respectively. Figure 9 illustrates the layout of the designed dual frequency BPD using the π-shaped matching transformer.

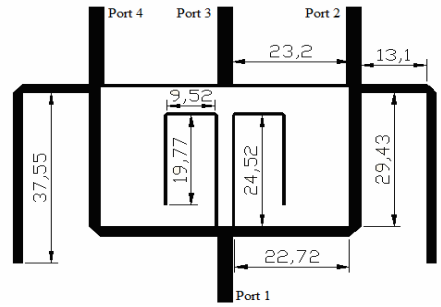

Figure 9. The layout of the dual-frequency BPD using the π-shaped matching network (All dimensions are in mm).

Figure 10 presents the simulation results of this dual-frequency 3-way BPD. Again, the dual-frequency behavior is very clear, with very good input port matching around the design frequencies. Figures 10(b) and 10(c) show also that the transmission parameters are close to their theoretical values at the design frequencies.

5. FABRICATED DIVIDERS AND MEASUREMENT RESULTS

The dual-frequency BPDs, presented above, have been fabricated using the same FR-4 substrate, mentioned earlier, and tested using an Agilent Spectrum Analyzer (with a built-in tracking generator extending from 0–1.5 GHz). Figures 11–13 show photographs of the three fabricated dual-frequency dividers. From these figures, it can be seen that the BPD that incorporates the π-shaped matching network has the least area. Specifically, ignoring the lengths of the feeding lines, the BPD with the two-section TLT occupies an area of approximately 35 cm^2, while the one with the T-shaped matching network occupies an area of approximately 88 cm^2, and the one with the π-shaped matching network occupies an area of approximately 33 cm^2. It should be mentioned that significant reduction in the areas of the three circuits can still be achieved by using meandered lines and/or printing the stubs inside the empty area of the divider.

Figure 14 presents the measurement results for the dual-frequency 3-way BPD using TLT sections. These results are in good agreement with the simulated ones shown in Figure 6. The measured matching parameter S_{11} equals -25 dB and -27 dB at 0.5 GHz and 1 GHz, respectively, and the transmission parameters are around -5 dB at the design frequencies.

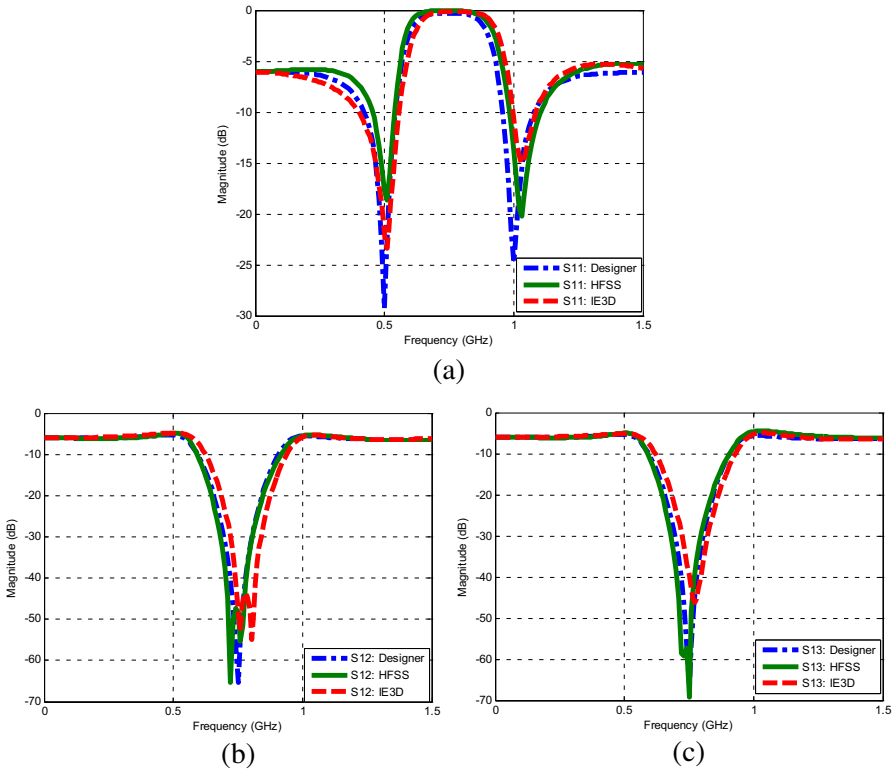

Figure 10. The simulation results for the dual-frequency BPD using π-shaped matching network.

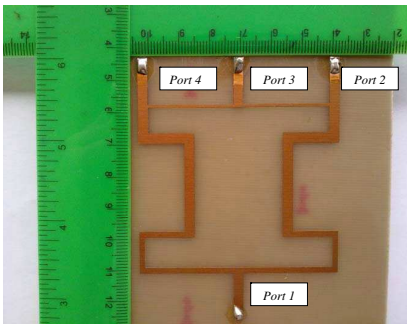

Figure 11. A picture of the dual-frequency 3-way BPD using the two-section TLT.

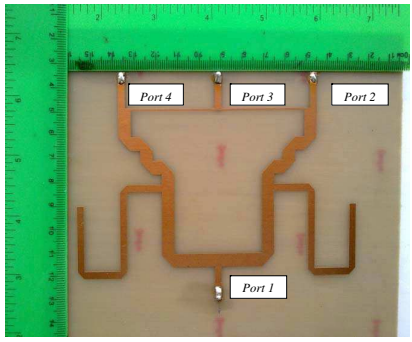

Figure 12. A picture of the dual-frequency 3-way BPD using the T-shaped matching network.

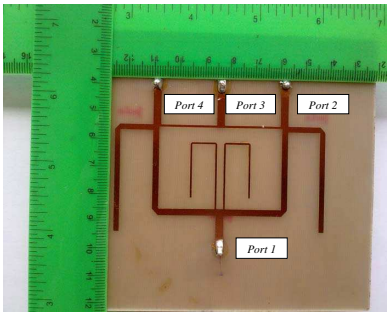

Figure 13. A picture of the dual-frequency 3-way BPD using the π-shaped matching network.

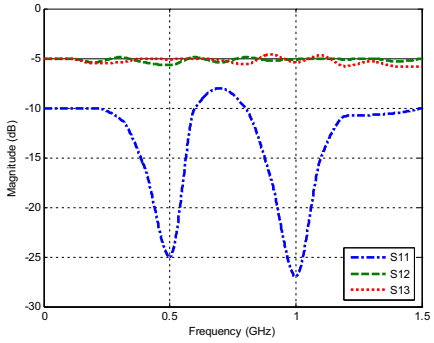

Figure 14. The measurement results for the dual-frequency BPD using TLT sections.

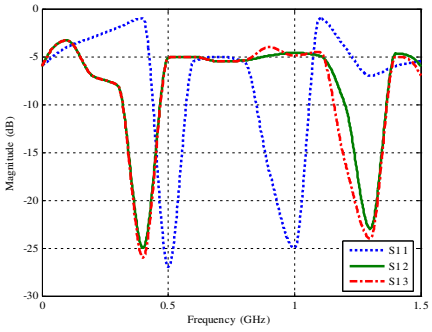

Figure 15. The measurement results for the dual-frequency BPD using T-shaped matching network.

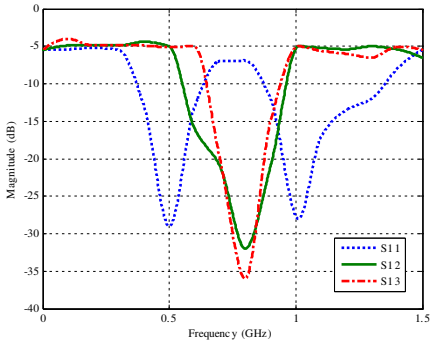

Figure 16. The measurement results for the dual-frequency BPD using π-shaped matching network.

Table 1. Comparison between the three BPDs.

Measured values	S_{11} (dB)		S_{12} (dB)		S_{13} (dB)		Area (cm^2)
Frequency (GHz)	0.5	1	0.5	1	0.5	1	—
Two-section BPD	−25	−27	−5.7	−5.09	−5.7	−5.4	35
T-Shaped BPD	−26.9	−25.3	−5.09	−4.6	−5.09	−4.9	88
π−Shaped BPD	−29.1	−27.7	−5.01	−5.1	−5.01	−5.1	33

Figure 15 shows the measurement results for the dual-frequency 3-way BPD when a T-shaped matching network is used while Figure 16 shows the measurement results for the divider with π-shaped matching network. For both dividers, input port matching parameter S_{11} of about -25 dB is achieved at the design frequencies, and acceptable transmission parameters are obtained. The discrepancies between simulation and measurement results could be due to the connectors, fabrication and measurement errors, and the fact that a Spectrum Analyzer (not a Network Analyzer) was used.

Table 1 summarizes the results of the three fabricated BPDs. From this table the fabricated BPDs reveal good performances at both design frequencies. The π-Shaped BPD gives the least occupied PCB area, compared to the other fabricated BPD.

6. CONCLUSION

Three dual-frequency matching networks were investigated and applied in the design of dual-frequency modified 3-way Bagley power dividers. Dual-frequency operation was achieved using two sections of TLTs, T-shaped matching network, and π-shaped matching network. Both the full-wave simulation results and the experimental results confirmed the dual-frequency operation of the designed dividers. Very good input port matching and transmission responses were obtained at the design frequencies. Differences between the simulations and measurements results could be due to the fabrication process, and measurements errors. Even though a 3-way BPD was only considered in this paper, the same procedure can be applied on BPDs with any (odd) number of output ports.

REFERENCES

1. Monzon, C., "A small dual-frequency transformer in two sections," *IEEE Transactions on Microwave Theory and Techniques*, Vol. 15, No. 4, 1157–1161, Apr. 2003.
2. Chongcheawchamnan, M., S. Patissang, and S. Srisathit, "Analysis and design of a three section transmission line-transformer," *IEEE Transactions on Microwave Theory and Techniques*, Vol. 53, No. 7, 2458–2462, Jul. 2005.
3. Jwaied, H., F. Muwanes, and N. Dib, "Analysis and design of quad-band four-section transmission line impedance transformer," *Applied Computational Electromagnetics Society (ACES) Journal*, Vol. 22, No. 3, 381–387, Nov. 2007.

4. Khodier, M., N. Dib, and J. Ababneh, "Design of multi-band multi-section transmission line transformer using particle swarm optimization," *Electrical Engineering Journal (Archiv fur Elektrotechnik)*, Vol. 90, No. 4, 293–300, Apr. 2008.
5. Mohra, A. and M. Alkanhal, "Dual band Wilkinson power dividers using T-sections," *Journal of Microwaves, Optoelectronics and Electromagnetic Applications,* Vol. 7, No. 2, 83–90, 2008.
6. Wu, Y., Y. Liu, and S. Li, "A compact Pi-structure dual band transformer," *Progress In Electromagnetics Research*, Vol. 88, 121–134, 2008.
7. Feng, C., G. Zhao, X. Liu, and F. Zhang, "A novel dual-frequency unequal Wilkinson power divider," *Microwave and Optical Technology Letters,* Vol. 50, No. 6, 1695–1699, Jun. 2008.
8. Chongcheawchamnan, M., S. Patissang, M. Krairiksh, and I. Robertson, "Tri-band Wilkinson power divider using a three-section transmission-line transformer," *IEEE Microwave and Wireless Communications Letters*, Vol. 16, No. 8, 452–454, Aug. 2006.
9. Jwaied, H., F Mawanes, and N. Dib, "Analysis and design of a quad-band Wilkinson power divider," *Int. Journal on Wireless and Optical Communication*, Vol. 4, No. 3, 305–312, 2007.
10. Dib, N. and M. Khodier, "Design and optimization of multi-band Wilkinson power divider," *International Journal of RF and Microwave Computer-aided Engineering*, Vol. 18, No. 1, 14–20, Jan. 2008.
11. Qaroot, A. M., N. I. Dib, and A. A. Gheethan, "Design methodology of multi-frequency un-equal split Wilkinson power divider using transmission line transformers," *Progress In Electromagnetics Research B*, Vol. 22, 1–21, 2010.
12. Chin, K., K. Lin, Y. Wei, T. Tseng, and Y. Yang, "Compact dual-band branch-line and rat-race couplers with stepped-impedance-stub lines," *IEEE Transactions on Microwave Theory and Techniques*, Vol. 58, No. 5, May 2010.
13. Niu, J.-X. and X.-L. Zhou, "A novel dual-band branch line coupler based on strip-shaped complementary split ring resonators," *Microwave and Optical Technology Letters,* Vol. 49, No. 11, 2859–2862, Nov. 2007.
14. Cheng, K.-K. and F. Wong, "A novel approach to the design and implementation of dual-band compact planar 90 branch-line coupler," *IEEE Transactions on Microwave Theory and Techniques*, Vol. 52, No. 11, 2458–2463, Nov. 2004.

15. Hayati, M. and M. Nosrati, "Loaded coupled transmission line approach of left handed (LH) structures and realization of a highly compact dual-band branchline coupler," *Progress In Electromagnetics Research C*, Vol. 10, 75–86, 2009.
16. Wu, Y., Y. Liu, and S. Li, "A new dual-frequency Wilkinson power divider," *Journal of Electromagnetic Waves and Applications*, Vol. 23, No. 4, 483–492, 2009.
17. Li, X., S.-X. Gong, L. Yang, and Y.-J. Yang, "A novel Wilkinson power divider for dual-band operation," *Journal of Electromagnetic Waves and Applications* Vol. 23, No. 2–3, 395–404, 2009.
18. Li, Q., J.-G. Gong, C.-L. Li, X.-H. Wang, L. Xu, and X.-W. Shi, "A compact dual-frequency threeway unequal power divider," *Journal of Electromagnetic Waves and Applications*, Vol. 24, No. 2–3, 383–390, 2010.
19. Wu, Y., Y. Liu, S. Li, C. Yu, and X. Liu, "Closed-form design method of an N-way dual-band Wilkinson hybrid power divider," *Progress In Electromagnetics Research*, Vol. 101, 97–114, 2010.
20. Yang, T., C. Liu, L. Yan, and K. Huang, "A compact dual-band power divider using planar artificial transmission lines for GSM/DCS applications," *Progress In Electromagnetics Research Letters*, Vol. 10, 185–191, 2009.
21. Wuren, T., K. Taniya, I. Sakagami, and M. Tahara, "Miniaturization of 3- and 5-way bagley polygon power dividers," *Asia-Pacific Microwave Conference (APMC) Proceedings*, Vol. 4, Dec. 2005.
22. Oraizi, H. and S. A. Ayati, "Optimum design of a modified 3-way bagley rectangular power divider," *2010 Mediterranean Microwave Symposium (MMS)*, 25–28, 2010.
23. Sakagami, I., T. Wuren, M. Fujii, and M. Tahara, "Compact multi-way power dividers similar to the bagley polygon," *2007 IEEE/MTT-S Int. Microwave Symposium*, 419–422, 2007.
24. Elles, D. and Y. K. Yoon, "Compact dual band three way bagley polygon power divider using composite right/left handed (CRLH) transmission lines," *2009 IEEE/MTT-S Int. Microwave Symposium*, 485–488, 2009.
25. Gomez-Garcia, R. and M. Sanchez-Renedo, "Application of generalized bagley-polygon four-port power dividers to designing microwave dual-band bandpass planar filters," *2010 IEEE/MTT-S Int. Microwave Symposium*, 580–583, 2010.
26. Ansoft Corporation, www.ansoft.com.
27. Zeland software, www.zeland.com.